

Multi-line diagnostics of the axi-symmetric wind around the MS-type AGB star RS Cancri

Jan Martin Winters^{1,*}, Thibaut Le Bertre², Do Thi Hoai³, Ka Tat Wong¹, Pham Tuyet Nhung³, Pierre Lesaffre⁴, Wonju Kim⁵, and Pierre Darriulat³

¹IRAM, 300 rue de la Piscine, 38406 St. Martin d'Hères, France

²LERMA, Observatoire de Paris, 61 av. de l'Observatoire, 75014 Paris, France

³VNSC, VAST, 18 Hoang Quoc Viet, Cau Giay, Ha Noi, Viet Nam

⁴LPENS, 24 rue Lhomond, 75231 Paris, France

⁵I. Physikalisches Institut, Uni Köln, Zùlpicher Str. 77, 50937 Köln, Germany

Abstract. We present data recently obtained with NOEMA/PolyFiX on the MS-type Asymptotic Giant Branch (AGB) star RS Cnc, allowing to characterize in detail the structure of its wind. These results became possible by the recent advances of the NOEMA observatory, which combine large spectral bandwidth with high sensitivity together with still increasing spatial resolution.

1 Introduction

We observed the largely unexplored intermediate type AGB star RS Cnc, a star already mixing Carbon up to its photosphere by the third dredge-up process. It is a relatively nearby semi-regular variable star ($d = 150$ pc) with a stellar temperature on the upper end for an AGB star ($T_{\star} = 3200$ K). It develops a wind with a low terminal outflow speed of 8 km s^{-1} and a relatively low mass loss rate of the order of $10^{-7} M_{\odot} \text{ yr}^{-1}$. Until our work, only CO, SiO and HI were detected in the mm to radio range in this object (see, e.g., [1, 2]).

We picked RS Cnc because of its peculiar CO line profiles, which are composed of a broad pedestal with a super-imposed narrow central component (Fig. 1, right). An early interpretation of this kind of composite line profiles was given by [3] in terms of successive winds with different mass-loss rate and different outflow velocity, whereas [1] proposed an interpretation for RS Cnc in terms of a bipolar outflow with an equatorial enhanced density structure.

2 Results

2.1 Molecular lines

A frequency range of 32 GHz in the 1 mm band was covered with two spectral setups using NOEMA's wideband correlator PolyFiX to observe diagnostically useful lines of CO and SiO, but also other interesting lines, e.g., from HCN and H₂O. In the end, we detect many more species than expected, including their isotopologs, i.e., SO, SO₂, ³⁴SO, vibrationally excited H₂O, Si¹⁷O, ²⁹SiO, HCN, H¹³CN, and even PN. In total, we detect 32 lines, emitted by 13 molecules and isotopologs, of which the latter nine species are first detections in RS Cnc in the mm range. All details of the observations are given in [4].

*e-mail: winters@iram.fr

2.2 Morpho-kinematics of the wind

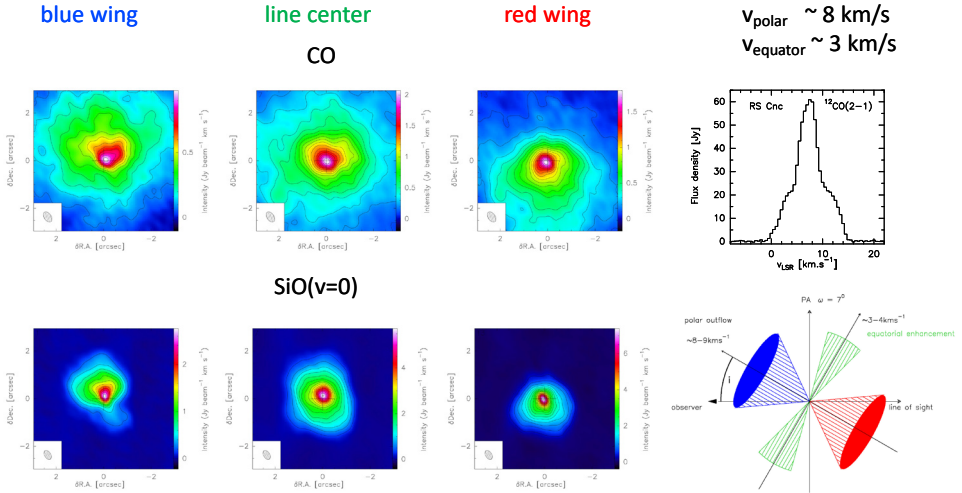


Figure 1. Integrated intensity maps in CO(2-1) and SiO(v=0,6-5) (left), CO(2-1) line profile (upper right), and sketch of the outflow structure (lower right).

In particular from CO, but also from SiO, information is obtained on the morpho-kinematic structure of the large-scale outflow. In Fig. 1 we show integrated intensity maps of the blue line wing, the line center, and the red line wing of CO(2-1) on top and of SiO(6-5) on the bottom row. In both lines, our modeling reveals a bipolar structure expanding at $\sim 8 \text{ km s}^{-1}$ toward us in the North and receding in the South, plus an equatorial enhanced density structure expanding at a much lower speed of $\sim 3 \text{ km s}^{-1}$. We note that SiO particularly probes the inner parts of the circumstellar shell whereas CO extends much farther outward.

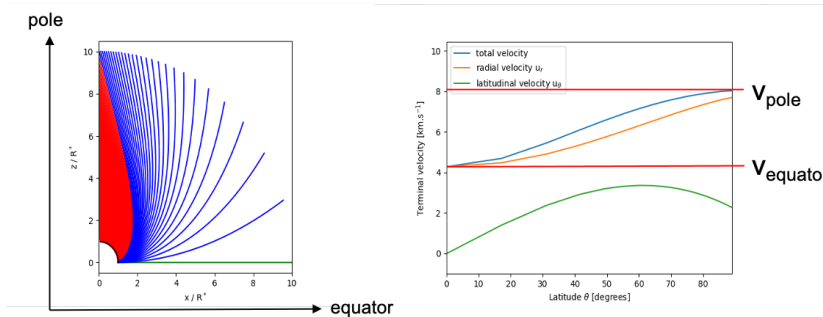


Figure 2. Toroidal magnetic field: resulting parcel trajectories in the $x-z$ plane (left) and wind velocities versus stellar latitude (right).

A convenient interpretation of this outflow structure would be in terms of a companion. However, no companion has been detected in RS Cnc by now (which does not exclude the presence of one). More importantly, a companion would not easily explain the velocity structure, showing higher velocities toward the poles than toward the equator. We therefore propose an

alternative interpretation in terms of a toroidal magnetic field that would funnel material toward the poles and at the same time would naturally provide outflow velocities that are small at the equator and increase toward the polar direction due to acceleration by the Lorentz force. Figure 2 presents a simplified model of a magnetized wind in such a scenario.

2.3 Rotating structure

Zooming into smaller scales, as probed by multiple species such as SO₂, HCN, SO, and (v=1) vibrationally excited lines of SiO, we find a velocity structure rotated by 90° with respect to the bipolar outflow and with velocities of the order of ±1 km s⁻¹. Figure 4, left plot shows the first-moment map of HCN emission. We interpret this velocity pattern in terms of rotation.

2.4 Broad line wings - photospheric shocks?: The innermost region

From SiO we detect several lines in different vibrational states up to v=2 and from several isotopes, a gallery of some of those is shown in Fig. 3. It is worth noting that the SiO(v=1,J=5-4) line was masing in 2017 around light minimum. However, in 2020, about 3.2 cycles later, the maser had disappeared. Temporal variations of SiO masers are quite common for pulsating AGB stars, but that the maser completely disappeared came as a surprise.

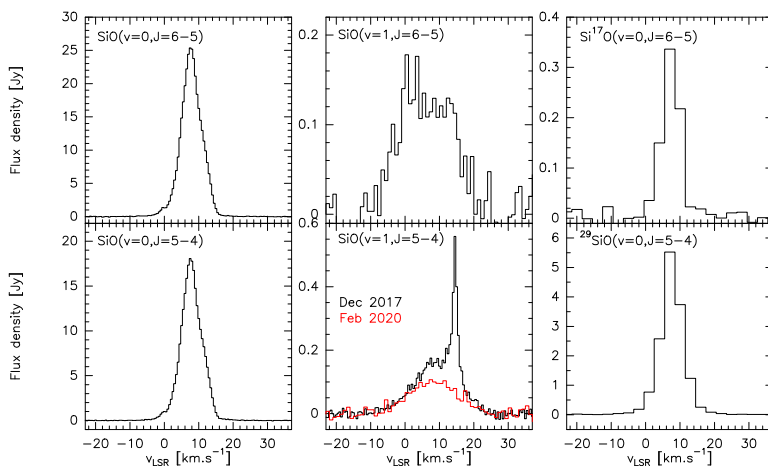


Figure 3. Gallery of detected SiO lines.

A striking feature of the SiO lines is their broad wings that indicate velocities almost twice as high as the maximum velocities seen in CO: this has been seen in many other similar stars, like EP Aqr ([5]), R Dor ([6]), and in most of the stars covered by the ALMA large program ATOMIUM on AGB stars ([7]). The map in the right plot of Fig. 4 displays the outflow velocity versus projected distance from the line of sight toward the star, showing that these high velocities only occur close to the central line of sight, i.e. very close to the star (the black line indicates the polar outflow velocity measured on the CO lines). As this type of velocity distribution is seen in many stars, and independent of the orientation of a possible symmetry axis with respect to the line of sight, a common, non-directional mechanism is needed to explain it. Our interpretation is in terms of shocks produced by the stellar pulsation

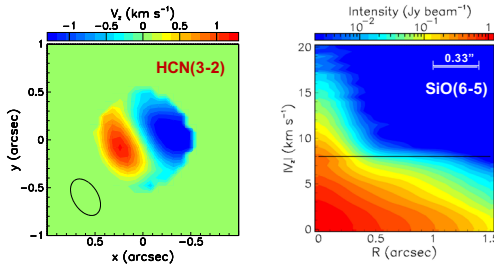


Figure 4. Left: Rotating structure as probed in HCN. Right: High velocities close to the line of sight toward the star as probed in SiO.

that provide high velocities close to the star but are damped out when traveling through the stellar atmosphere. These velocities can be higher than the final expansion velocity of the wind, as was already argued by [8] and [9] based on SiO maser observations, and discussed in [10, 11], based on hydrodynamic models.

3 Summary

With PolyFiX we detect nine new molecules and isotopologs in RS Cnc (see Sect. 2.1) that serve as detailed diagnostics of the star’s environment on very different spatial scales. We essentially confirm the bipolar outflow structure with an equatorial density enhancement. In addition we find a rotating region close to the star, as well as some high-velocity material in the innermost region, which likely indicates shocks traveling through the stellar atmosphere.

In the future we plan to investigate in more detail the role of magnetic fields in shaping the wind structure and to apply a more detailed radiative transfer modeling of the detected lines to better determine the thermodynamic structure of the shell and, in particular, the expected imprint of atmospheric shocks on the line profiles of the different molecular tracers.

In order to investigate, whether the velocity structure seen in HCN and other molecules really indicates rotation, we will propose to carry out observations with higher spatial resolution that may also reveal if the corresponding velocity pattern is Keplerian or not. These observations should become possible by the end of 2022 thanks to the upcoming extended baselines of NOEMA, providing a spatial resolution increased by a factor of two with respect to the current status presented here, and allowing us to resolve a region of about $20 R_*$ at RS Cnc’s distance. A direct probing of the potentially shocked regions however needs a much higher spatial resolution that may remain a dream for some while.

References

- [1] Y. Libert, J.M. Winters, T. Le Bertre, E. Gérard, L.D. Matthews, *A&A* **515**, A112 (2010)
- [2] P. de Vicente, V. Bujarrabal, A. Díaz-Pulido et al., *A&A* **589**, A74 (2016)
- [3] G.R. Knapp, K. Young, E. Lee, A. Jorissen, *ApJS* **117**, 209 (1998)
- [4] J.M. Winters, D.T. Hoai, K.T. Wong et al., *A&A* **658**, A135 (2022)
- [5] P. Tuan-Anh, D.T. Hoai, P.T. Nhung et al., *MNRAS* **487**, 622 (2019), 1905.02715
- [6] L. Decin, A.M.S. Richards, T. Danilovich, W. Homan, J.A. Nuth, *A&A* **615**, A28 (2018)
- [7] C.A. Gottlieb, L. Decin, A.M.S. Richards et al., *A&A* **660**, A94 (2022)
- [8] J. Cernicharo, J. Alcolea, A. Baudry, E. González-Alfonso, *A&A* **319**, 607 (1997)
- [9] F. Herpin, A. Baudry, J. Alcolea, J. Cernicharo, *A&A* **334**, 1037 (1998)
- [10] J.M. Winters, T. Le Bertre, K.S. Jeong, C. Helling, E. Sedlmayr, *A&A* **361**, 641 (2000)
- [11] J.M. Winters, T. Le Bertre, L.Å. Nyman, A. Omont, K.S. Jeong, *A&A* **388**, 609 (2002)